

# 3D AOA TARGET TRACKING WITH TWO-STEP INSTRUMENTAL-VARIABLE KALMAN FILTERING

Ngoc Hung Nguyen and Kutluyıl Doğançay

School of Engineering, University of South Australia, Mawson Lakes SA 5095, Australia

## ABSTRACT

A two-step pseudolinear Kalman filter (2S-PLKF) was previously proposed for angle-of-arrival (AOA) target tracking in three-dimensional space drawing on the pseudolinear rearrangement of nonlinear azimuth and elevation angle measurement equations. Despite enjoying low computational complexity, this algorithm suffers from a severe bias problem arising from the nonlinear-to-linear transformation of the angle measurement equations. This paper presents a new two-step instrumental-variable Kalman filter (2S-IVKF) exploiting the use of pseudolinear estimation, as well as instrumental-variable estimation to overcome the bias problem. The performance advantage of the proposed 2S-IVKF algorithm over the 2S-PLKF, as well as extended and sigma-point Kalman filters is demonstrated with simulation examples.

**Index Terms**— Angle of arrival (AOA), target tracking, pseudolinear Kalman filter (PLKF), instrumental-variable Kalman filter (IVKF), posterior Cramér-Rao lower bound (PCRLB).

## 1. INTRODUCTION

Angle-of-arrival (AOA) target tracking has been an important area of research for many years with applications in both civilian and military domains including wireless communications, navigation, radar and sonar. In this paper, we consider the problem of target tracking in three-dimensional (3D) space with a single moving sensor platform collecting azimuth and elevation angle measurements.

AOA target tracking is essentially a nonlinear state-space estimation problem due to the nonlinear relationship of the azimuth and elevation angle measurements with the true target position. The extended Kalman filter (EKF) was employed for AOA target tracking in the early works of [1, 2]. Several variants of EKF for AOA target tracking were also developed in the literature including the modified-polar EKF (EKF-MPC) [3] and the modified-spherical EKF (EKF-MS) [4–6]. The use of sigma-point algorithms such as the unscented Kalman filter (UKF) [7, 8] and cubature Kalman filter (CKF) [9] for AOA target tracking was reported in [10–12]. The particle filter was also considered for AOA target tracking (see, e.g., [13–15]), but its high computational complexity makes it less attractive for real-time operation [16].

For azimuth-only target tracking in two-dimensional (2D) plane, an alternative to nonlinear filtering is to consider a pseudolinear rearrangement of the nonlinear azimuth angle measurement equation so that the linear Kalman filter can be applied. This results in the so-called pseudolinear Kalman filter (PLKF) [1, 13, 17, 18]. In a broader context, the framework of pseudolinear estimation was widely used in the context of localization of a stationary target and motion analysis of a nonmaneuvering target [19–25]. The main advantage of the PLKF lies in its high stability and low computational complexity [13]. Compared to the particle and sigma-point Kalman filters,

the PLKF exhibits a similar tracking performance at a lower computational complexity [13, 17, 18]. However, the PLKF is known to suffer severely from bias [26, 27], which in turn can adversely degrade its tracking performance, due to the correlation between the measurement matrix and the pseudolinear noise variable. To overcome such a bias problem, the instrumental-variable Kalman filter (IVKF) was developed in [27] based on the replacement of measurement matrix with an instrumental variable (IV) matrix in the computation of Kalman filter gain. The PLKF for 2D azimuth-only target tracking has been extended to 3D AOA target tracking with azimuth and elevation angle measurements in [28], where a two-step PLKF (2S-PLKF) algorithm comprised of two separate PLKF trackers to estimate the target state components on the  $xy$ -plane and the  $z$ -axis was developed. Similar to the PLKF, the main drawback of the 2S-PLKF is that it produces severely biased estimates.

The main contribution of this paper is to develop a new two-step IVKF (2S-IVKF) algorithm for 3D AOA target tracking building on the developments in [27] and [28]. Specifically, the algorithm consists of two trackers operating in parallel, including an IVKF tracker for estimating the  $xy$ -state component and a PLKF tracker for estimating the  $z$ -state component of the target. Thanks to the use of instrumental variables, the 2S-IVKF enjoys the inherent robustness and computational effectiveness of the pseudolinear estimation approach while at the same time overcoming the severe bias problem that plagues the 2S-PLKF. The performance advantage of the proposed 2S-IVKF algorithm, i.e., producing a negligible bias and exhibiting a mean squared error close to the posterior Cramér-Rao lower bound, is demonstrated via numerical Monte Carlo simulations. It is observed from simulation results that the 2S-IVKF is more robust against noise than the EKF and EKF-MS. In addition, the 2S-IVKF exhibits a comparable tracking performance to the UKF and CKF while requiring much less computation.

## 2. PROBLEM FORMULATION

The problem of 3D AOA target tracking with a moving sensor platform using azimuth and elevation angle measurements is depicted in Fig. 1. At discrete-time instant  $k$ , the unknown target position and velocity are denoted by  $\mathbf{p}_k = [p_{x,k}, p_{y,k}, p_{z,k}]^T$  and  $\mathbf{v}_k = [v_{x,k}, v_{y,k}, v_{z,k}]^T$ , respectively, while the sensor position is denoted by  $\mathbf{r}_k = [r_{x,k}, r_{y,k}, r_{z,k}]^T$ . Here, the superscript  $T$  stands for matrix transpose. The dynamic model for the target state vector  $\mathbf{s}_k = [\mathbf{p}_k^T, \mathbf{v}_k^T]^T$  is given by

$$\mathbf{s}_k = \mathbf{F}\mathbf{s}_{k-1} + \mathbf{w}_{k-1} \quad (1)$$

where  $\mathbf{F}$  is the state transition matrix, and  $\mathbf{w}_{k-1} \sim \mathcal{N}(\mathbf{0}, \mathbf{Q})$  is the independent zero-mean Gaussian process noise with covariance  $\mathbf{Q}$ , which corresponds to unknown maneuvers of the target [29]. Under

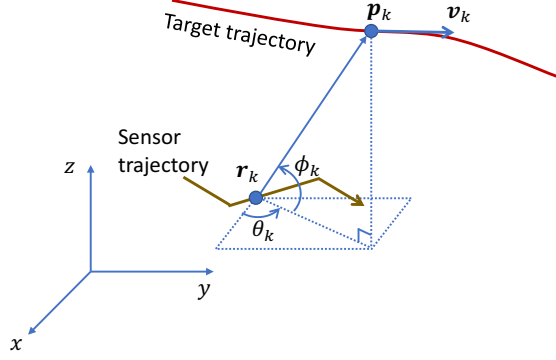


Fig. 1. 3D AOA target tracking geometry.

the assumption of nearly constant velocity dynamics, we have

$$\mathbf{F} = \begin{bmatrix} \mathbf{I}_{3 \times 3} & T\mathbf{I}_{3 \times 3} \\ \mathbf{0}_{3 \times 3} & \mathbf{I}_{3 \times 3} \end{bmatrix}, \quad \mathbf{Q} = \begin{bmatrix} \frac{T^3}{3}\mathbf{Q}_o & \frac{T^2}{2}\mathbf{Q}_o \\ \frac{T^2}{2}\mathbf{Q}_o & T\mathbf{Q}_o \end{bmatrix} \quad (2)$$

where  $T$  is the sampling interval, and  $\mathbf{Q}_o = \text{diag}(q_x, q_y, q_z)$  with  $q_x, q_y$  and  $q_z$  denoting the power spectral densities of the process noise in  $x$ -,  $y$ - and  $z$ -coordinates [29]. Here, and throughout the paper,  $\mathbf{0}$  and  $\mathbf{I}$  denote zero and identity matrices, respectively, whose dimensions are specified in the subscript.

At each time instant  $k$ , the sensor collects noisy azimuth and elevation angle measurements as

$$\tilde{\theta}_k = \theta_k + n_{\theta,k}, \quad \theta_k = \tan^{-1} \frac{p_{y,k} - r_{y,k}}{p_{x,k} - r_{x,k}} \quad (3a)$$

$$\tilde{\phi}_k = \phi_k + n_{\phi,k}, \quad \phi_k = \sin^{-1} \frac{p_{z,k} - r_{z,k}}{\|\mathbf{p}_k - \mathbf{r}_k\|} \quad (3b)$$

where  $n_{\theta,k} \sim \mathcal{N}(0, \sigma_{\theta,k}^2)$  and  $n_{\phi,k} \sim \mathcal{N}(0, \sigma_{\phi,k}^2)$  are independent zero-mean Gaussian random variables. The noise variables  $\mathbf{w}_k, n_{\theta,k}$  and  $n_{\phi,k}$  are statistically independent. Here,  $\tan^{-1}$  stands for the 4-quadrant arctangent and  $\|\cdot\|$  the Euclidean norm. Note that the noise variances  $\sigma_{\theta,k}^2$  and  $\sigma_{\phi,k}^2$ , assumed to be known *a priori*, can vary with time  $k$ .

The state-space model for the 3D AOA target tracking problem under consideration is given by

$$\mathbf{s}_k = \mathbf{F}\mathbf{s}_{k-1} + \mathbf{w}_{k-1} \quad (4a)$$

$$\tilde{\mathbf{f}}_k = \begin{bmatrix} \tilde{\theta}_k \\ \tilde{\phi}_k \end{bmatrix} = \mathbf{f}(\mathbf{s}_k) + \mathbf{n}_k = \begin{bmatrix} \theta_k(\mathbf{s}_k) \\ \phi_k(\mathbf{s}_k) \end{bmatrix} + \begin{bmatrix} n_{\theta,k} \\ n_{\phi,k} \end{bmatrix} \quad (4b)$$

The objective is to estimate the unknown target state vector  $\mathbf{s}_k$  at time instant  $k$  from a history of angle measurements  $\tilde{\mathbf{f}}_{0:k} = \{\tilde{\mathbf{f}}_0, \tilde{\mathbf{f}}_1, \dots, \tilde{\mathbf{f}}_k\}$  with an initial state estimate  $\hat{\mathbf{s}}_{0|-1} = \mathbb{E}\{\mathbf{s}_0\}$  and initial state covariance  $\mathbf{P}_{0|-1} = \mathbb{E}\{(\mathbf{s}_0 - \mathbb{E}\{\mathbf{s}_0\})(\mathbf{s}_0 - \mathbb{E}\{\mathbf{s}_0\})^T\}$ . This is a nonlinear state-space estimation problem since  $\mathbf{f}(\mathbf{s}_k)$  in the observation equation (4b) is a nonlinear function of  $\mathbf{s}_k$ .

### 3. TWO-STEP INSTRUMENTAL-VARIABLE KALMAN FILTER

The proposed 2S-IVKF algorithm consists of two trackers operating in parallel to estimate the  $xy$ - and  $z$ -components of the target state vector  $\mathbf{s}_k$ . In what follows, we provide the details of the algorithm.

#### 3.1. The IVKF tracker for the $xy$ -state vector

Let  $\mathbf{s}_{xy,k} = [p_{x,k}, p_{y,k}, v_{x,k}, v_{y,k}]^T$ ,  $\mathbf{p}_{xy,k} = [p_{x,k}, p_{y,k}]^T$  and  $\mathbf{r}_{xy,k} = [r_{x,k}, r_{y,k}]^T$  denote the  $xy$ -components of the target state vector  $\mathbf{s}_k$ , target position vector  $\mathbf{p}$  and receiver position vector  $\mathbf{r}$ , respectively, at time instant  $k$ . The dynamic model for  $\mathbf{s}_{xy,k}$  is thus given by

$$\mathbf{s}_{xy,k} = \mathbf{F}_{xy}\mathbf{s}_{xy,k-1} + \mathbf{w}_{xy,k-1} \quad (5)$$

where

$$\mathbf{F}_{xy} = \begin{bmatrix} \mathbf{I}_{2 \times 2} & T\mathbf{I}_{2 \times 2} \\ \mathbf{0}_{2 \times 2} & \mathbf{I}_{2 \times 2} \end{bmatrix}, \quad \mathbf{Q}_{xy} = \begin{bmatrix} \frac{T^3}{3}\mathbf{Q}_{xy,o} & \frac{T^2}{2}\mathbf{Q}_{xy,o} \\ \frac{T^2}{2}\mathbf{Q}_{xy,o} & T\mathbf{Q}_{xy,o} \end{bmatrix}. \quad (6)$$

Here,  $\mathbf{w}_{xy,k-1} \sim \mathcal{N}(\mathbf{0}, \mathbf{Q}_{xy})$  and  $\mathbf{Q}_{xy,o} = \text{diag}(q_x, q_y)$ .

The estimation of  $\mathbf{s}_{xy,k}$  is carried out utilizing the azimuth angle measurement  $\tilde{\theta}_k$ . The nonlinear azimuth equation (3a) can be rearranged into a pseudolinear equation as [20, 26]

$$\tilde{b}_{xy,k} = \mathbf{H}_{xy,k}\mathbf{s}_{xy,k} + \eta_{xy,k} \quad (7)$$

where  $\tilde{b}_{xy,k} = \tilde{\mathbf{u}}_{xy,k}^T \mathbf{r}_{xy,k}$ ,  $\mathbf{H}_{xy,k} = \tilde{\mathbf{u}}_{xy,k}^T \mathbf{M}_{xy}$  and  $\eta_{xy,k} = -\|\mathbf{d}_{xy,k}\| \sin n_{\theta,k}$  with  $\tilde{\mathbf{u}}_{xy,k} = [\sin \theta_k, -\cos \theta_k]^T$ ,  $\mathbf{M}_{xy} = [\mathbf{I}_{2 \times 2}, \mathbf{0}_{2 \times 2}]$  and  $\mathbf{d}_{xy,k} = \mathbf{p}_{xy,k} - \mathbf{r}_{xy,k}$ . The pseudolinear noise covariance is given by  $R_{xy,k} = \mathbb{E}\{\eta_{xy,k}^2\} = \|\mathbf{d}_{xy,k}\|^2 \mathbb{E}\{\sin^2 n_{\theta,k}\} \approx \|\mathbf{d}_{xy,k}\|^2 \sigma_{\theta,k}^2$  for sufficiently small noise.

Equations (5) and (7) together form a pseudolinear state-space estimation problem that can be solved by the IVKF algorithm [27]:

#### Phase 1 - Pseudolinear Kalman estimation:

$$\begin{aligned} \hat{\mathbf{s}}_{xy,k|k-1} &= \mathbf{F}_{xy}\hat{\mathbf{s}}_{xy,k-1|k-1} \\ \mathbf{P}_{xy,k|k-1} &= \mathbf{F}_{xy}\mathbf{P}_{xy,k-1|k-1}\mathbf{F}_{xy}^T + \mathbf{Q}_{xy} \\ R_{xy,k} &= \|\mathbf{M}_{xy}\hat{\mathbf{s}}_{xy,k|k-1} - \mathbf{r}_{xy,k}\|^2 \sigma_{\theta,k}^2 \\ \mathbf{K}_{xy,k} &= \mathbf{P}_{xy,k|k-1}\mathbf{H}_{xy,k}^T \\ &\quad \times (R_{xy,k} + \mathbf{H}_{xy,k}\mathbf{P}_{xy,k|k-1}\mathbf{H}_{xy,k}^T)^{-1} \\ \hat{\mathbf{s}}_{xy,k|k} &= \hat{\mathbf{s}}_{xy,k|k-1} + \mathbf{K}_{xy,k}(\tilde{b}_{xy,k} - \mathbf{H}_{xy,k}\hat{\mathbf{s}}_{xy,k|k-1}) \\ \mathbf{P}_{xy,k|k} &= \mathbf{P}_{xy,k|k-1} - \mathbf{K}_{xy,k}\mathbf{H}_{xy,k}\mathbf{P}_{xy,k|k-1}. \end{aligned} \quad (8)$$

#### Phase 2 - Bias compensation:

$$\hat{\mathbf{s}}_{xy,k|k}^{\text{BC}} = \hat{\mathbf{s}}_{xy,k|k} + \mathbf{P}_{xy,k|k}R_{xy,k}^{-1}\sigma_{\theta,k}^2\mathbf{M}_{xy}^T(\mathbf{M}_{xy}\hat{\mathbf{s}}_{xy,k|k} - \mathbf{r}_{xy,k}). \quad (9)$$

#### Phase 3 - IV estimation:

$$\begin{aligned} \hat{\theta}_{k|k}^{\text{BC}} &= \tan^{-1}((\hat{\mathbf{s}}_{xy,k|k}^{\text{BC}}(2) - r_{y,k}) / (\hat{\mathbf{s}}_{xy,k|k}^{\text{BC}}(1) - r_{x,k})) \\ \text{if } |\hat{\theta}_{k|k}^{\text{BC}} - \tilde{\theta}_k| &< \alpha_{\theta,k} \text{ and } k \geq k^\dagger \\ \mathbf{G}_{xy,k} &= [\sin \hat{\theta}_{k|k}^{\text{BC}}, -\cos \hat{\theta}_{k|k}^{\text{BC}}]\mathbf{M}_{xy} \\ \mathbf{K}_{xy,k}^{\text{IV}} &= \mathbf{P}_{xy,k|k-1}\mathbf{G}_{xy,k}^T(R_{xy,k} + \mathbf{H}_{xy,k}\mathbf{P}_{xy,k|k-1}\mathbf{G}_{xy,k}^T)^{-1} \\ \hat{\mathbf{s}}_{xy,k|k}^{\text{IV}} &= \hat{\mathbf{s}}_{xy,k|k-1} + \mathbf{K}_{xy,k}^{\text{IV}}(\tilde{b}_{xy,k} - \mathbf{H}_{xy,k}\hat{\mathbf{s}}_{xy,k|k-1}) \\ \mathbf{P}_{xy,k|k}^{\text{IV}} &= \mathbf{P}_{xy,k|k-1} - \mathbf{K}_{xy,k}^{\text{IV}}\mathbf{H}_{xy,k}\mathbf{P}_{xy,k|k-1} \\ \text{else} \\ \hat{\mathbf{s}}_{xy,k|k}^{\text{IV}} &= \hat{\mathbf{s}}_{xy,k|k}^{\text{BC}} \\ \mathbf{P}_{xy,k|k}^{\text{IV}} &= \mathbf{P}_{xy,k|k}. \end{aligned} \quad (10)$$

The initial state estimate  $\hat{\mathbf{s}}_{xy,0|-1}$  and covariance  $\mathbf{P}_{xy,0|-1}$  are extracted from the  $xy$ -components of  $\hat{\mathbf{s}}_{0|-1}$  and  $\mathbf{P}_{0|-1}$ , respectively.

The pseudolinear Kalman estimation (8) is simply a direct application of the linear Kalman filter to the pseudolinear state-space model consisting of (5) and (7). However, the state estimate  $\hat{\mathbf{s}}_{xy,k|k}$  obtained from (8) is biased predominantly due to the correlation between the measurement matrix  $\mathbf{H}_{xy,k}$  and the pseudolinear noise  $\eta_{xy,k}$  as a result of the transformation of the nonlinear azimuth equation (3a) into the pseudolinear form (7) [27]. In order to reduce this bias, a bias compensation step is performed by estimating and subtracting the bias of  $\hat{\mathbf{s}}_{xy,k|k}$  as in (9). Finally, the bias problem is resolved by the IV estimation step in a more effective manner. The main idea here is to replace the measurement matrix  $\mathbf{H}_{xy,k}^T$  with the IV matrix  $\mathbf{G}_{xy,k}^T$ , which is approximately uncorrelated with  $\eta_{xy,k}$  in the Kalman gain computation step. In particular, the bias-compensated state estimate  $\hat{\mathbf{s}}_{xy,k|k}^{\text{BC}}$  is utilized in the construction of  $\mathbf{G}_{xy,k}$  to approximate the noise-free version of  $\mathbf{H}_{xy,k}$ . Note that, the IV estimation step is performed in a selective manner (often known as the selective-angle-measurement (SAM) approach [19, 27]) to maintain a strong correlation between  $\mathbf{G}_{xy,k}$  and  $\mathbf{H}_{xy,k}$  as a requisite condition of IV estimation.

### 3.2. The PLKF tracker for the $z$ -state vector

The dynamic model of the  $z$ -component  $\mathbf{s}_{z,k} = [p_{z,k}, v_{z,k}]^T$  of the target state vector  $\mathbf{s}_k$  is given by

$$\mathbf{s}_{z,k} = \mathbf{F}_z \mathbf{s}_{z,k-1} + \mathbf{w}_{z,k-1} \quad (11)$$

where  $\mathbf{w}_{z,k-1} \sim \mathcal{N}(\mathbf{0}, \mathbf{Q}_z)$ . Here,  $\mathbf{F}_z$  and  $\mathbf{Q}_z$  are given by

$$\mathbf{F}_z = \begin{bmatrix} 1 & T \\ 0 & 1 \end{bmatrix}, \quad \mathbf{Q}_z = q_z \begin{bmatrix} \frac{T^3}{2} & \frac{T^2}{2} \\ \frac{T^2}{2} & T \end{bmatrix}. \quad (12)$$

By utilizing the  $xy$ -state estimate  $\hat{\mathbf{s}}_{xy,k|k}^{\text{IV}}$  and the elevation angle measurement  $\tilde{\phi}_k$ , the nonlinear elevation equation (3b) can be written in a pseudolinear form as

$$\tilde{b}_{z,k} = \mathbf{H}_{z,k} \mathbf{s}_{z,k} + \eta_{z,k} \quad (13)$$

where  $\tilde{b}_{z,k} = \|\mathbf{M}_{xy} \hat{\mathbf{s}}_{xy,k|k}^{\text{IV}} - \mathbf{r}_{xy,k}\| \tan \tilde{\phi}_k + r_{z,k}$ ,  $\mathbf{H}_z = [1, 0]$  and  $\eta_{z,k} = (\|\mathbf{p}_k - \mathbf{r}_k\| \sin n_{\phi,k} + (\|\mathbf{M}_{xy} \hat{\mathbf{s}}_{xy,k|k}^{\text{IV}} - \mathbf{r}_{xy,k}\| - \|\mathbf{d}_{xy,k}\|) \sin \tilde{\phi}_k) / \cos \tilde{\phi}_k$ .

Since  $\hat{\mathbf{s}}_{xy,k|k}^{\text{IV}}$  is an estimate with negligible bias thanks to the use of IV estimation, the elevation pseudolinear noise  $\eta_{z,k}$  is approximately zero-mean. In addition, the measurement matrix  $\mathbf{H}_z$  is deterministic, thus there is no correlation issue between  $\mathbf{H}_z$  and  $\eta_{z,k}$ , unlike their  $xy$ -counterparts. Given these facts, the  $z$ -state vector  $\mathbf{s}_{z,k}$  can be effectively estimated by applying the PLKF approach without posing any bias problems. Specifically, applying the linear Kalman filter to the pseudolinear state-space model consisting of (11) and (13) results in the following PLKF:

$$\begin{aligned} \hat{\mathbf{s}}_{z,k|k-1} &= \mathbf{F}_z \hat{\mathbf{s}}_{z,k-1|k-1} \\ \mathbf{P}_{z,k|k-1} &= \mathbf{F}_z \mathbf{P}_{z,k-1|k-1} \mathbf{F}_z^T + \mathbf{Q}_z \\ \mathbf{K}_{z,k} &= \mathbf{P}_{z,k|k-1} \mathbf{H}_{z,k}^T (\mathbf{R}_{z,k} + \mathbf{H}_{z,k} \mathbf{P}_{z,k|k-1} \mathbf{H}_{z,k}^T)^{-1} \\ \hat{\mathbf{s}}_{z,k|k} &= \hat{\mathbf{s}}_{z,k|k-1} + \mathbf{K}_{z,k} (\tilde{b}_{z,k} - \mathbf{H}_{z,k} \hat{\mathbf{s}}_{z,k|k-1}) \\ \mathbf{P}_{z,k|k} &= \mathbf{P}_{z,k|k-1} - \mathbf{K}_{z,k} \mathbf{H}_{z,k} \mathbf{P}_{z,k|k-1}. \end{aligned} \quad (14)$$

where the initial state estimate  $\hat{\mathbf{s}}_{z,0|0}$  and covariance  $\mathbf{P}_{z,0|0}$  are extracted from the  $z$ -components of  $\hat{\mathbf{s}}_{0|0}$  and  $\mathbf{P}_{0|0}$ , respectively. Here, the pseudolinear noise covariance  $\mathbf{R}_{z,k} = \mathbb{E}\{\eta_{z,k}\}$  is calculated from  $\tilde{\phi}_k$ ,  $\hat{\mathbf{s}}_{xy,k|k}^{\text{IV}}$  and  $\mathbf{P}_{xy,k|k}^{\text{IV}}$  as follows.

The elevation pseudolinear noise  $\eta_{z,k}$  in (13) can be written as

$$\eta_{z,k} = g_k(\tilde{\phi}_k, \hat{\mathbf{s}}_{xy,k|k}^{\text{IV}}(1), \hat{\mathbf{s}}_{xy,k|k}^{\text{IV}}(2)) - g_k(\phi_k, p_{x,k}, p_{y,k}) \quad (15)$$

where  $g_k(\phi_k, p_{x,k}, p_{y,k}) = \|\mathbf{p}_{xy,k} - \mathbf{r}_{xy,k}\| \tan \phi_k$ . For sufficiently small noise, the covariance  $\mathbf{R}_{z,k} = \mathbb{E}\{\eta_{z,k}\}$  can be approximated by

$$\mathbf{R}_{z,k} = \mathbf{\Gamma}_k \mathbf{\Lambda}_k \mathbf{\Gamma}_k^T \quad (16)$$

where

$$\mathbf{\Gamma}_k = \begin{bmatrix} \frac{\partial g_k}{\partial \phi_k} & \frac{\partial g_k}{\partial p_{x,k}} & \frac{\partial g_k}{\partial p_{y,k}} \end{bmatrix} \quad (17a)$$

$$\mathbf{\Lambda}_k = \begin{bmatrix} \sigma_{\tilde{\phi},k}^2 & 0 & 0 \\ 0 & \mathbf{P}_{xy,k|k}^{\text{IV}}(1,1) & \mathbf{P}_{xy,k|k}^{\text{IV}}(1,2) \\ 0 & \mathbf{P}_{xy,k|k}^{\text{IV}}(2,1) & \mathbf{P}_{xy,k|k}^{\text{IV}}(2,2) \end{bmatrix}. \quad (17b)$$

The Jacobian matrix  $\mathbf{\Gamma}_k$  is calculated using  $\tilde{\phi}_k$ ,  $\hat{\mathbf{s}}_{xy,k|k}^{\text{IV}}(1)$  and  $\hat{\mathbf{s}}_{xy,k|k}^{\text{IV}}(2)$ . The derivative terms in  $\mathbf{\Gamma}_k$  are straightforward to derive and their expressions are omitted here for brevity.

## 4. SIMULATIONS

This section presents a performance evaluation of the proposed 2S-IVKF algorithm in comparison with the EKF, EKF-MS, UKF, CKF and 2S-PLKF via Monte Carlo simulations. The posterior Cramér-Rao lower bound (PCRLB) [27, 30, 31] is also included as a theoretical performance benchmark. A 3D underwater tracking scenario is considered as depicted in Fig. 2, where a moving ownship tracks an autonomous underwater vehicle. The ownship travels on the  $xy$ -plane at a constant speed of 31.34 knots following a five-leg trajectory starting from  $[240, 0, 0]^T$  m at velocity of  $[-16, 2, 0]^T$  m/s. The leg length is 241.9 m and the angle between two consecutive legs is  $165.8^\circ$ . A total of  $N = 150$  azimuth/elevation measurements are collected by the ownship along its trajectory at  $t_k = kT$  (with  $T = 0.5$  s) for  $k = 0, 1, \dots, 149$ . The measurement noise is assumed to be i.i.d. with  $\sigma_{\theta,k} = \sigma_{\phi,k} = \sigma$ . The initial position and velocity of the target are  $\mathbf{p}_0 = [120, 168, 100]^T$  m and  $\mathbf{v}_0 = [0, 10, 3.6]^T$  m/s, respectively (i.e., roughly 20.66 knots in speed). The process noise power spectral densities are set to  $q_x = q_y = q_z = 0.01$  m<sup>2</sup>/s<sup>3</sup>. A Gaussian distribution around  $\mathbf{x}_0$  with covariance  $\mathbf{P}_{0|0} = \rho^2 \text{diag}(8^2, 8^2, 8^2, 0.4^2, 0.4^2, 0.4^2)$  is used to generate the initial track estimate  $\hat{\mathbf{x}}_{0|0}$  where  $\rho = \sigma$ . For the 2S-IVKF, we set  $\alpha_{\theta,k} = 4\sigma$  and  $k^\dagger = 40$ . The UKF parameters are set to  $\alpha^{\text{UKF}} = 0.5$ ,  $\kappa^{\text{UKF}} = 0$  and  $\beta^{\text{UKF}} = 2$ .

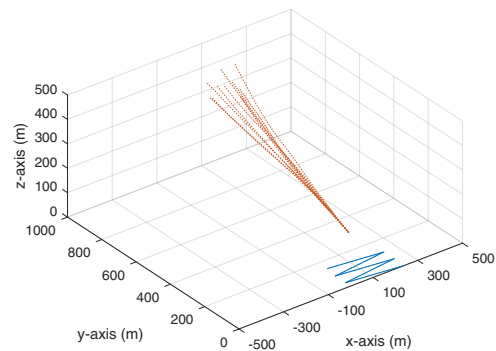


**Fig. 2.** Simulated tracking scenario: sensor trajectory (blue solid line) and 10 realizations of target trajectory (orange dotted lines).

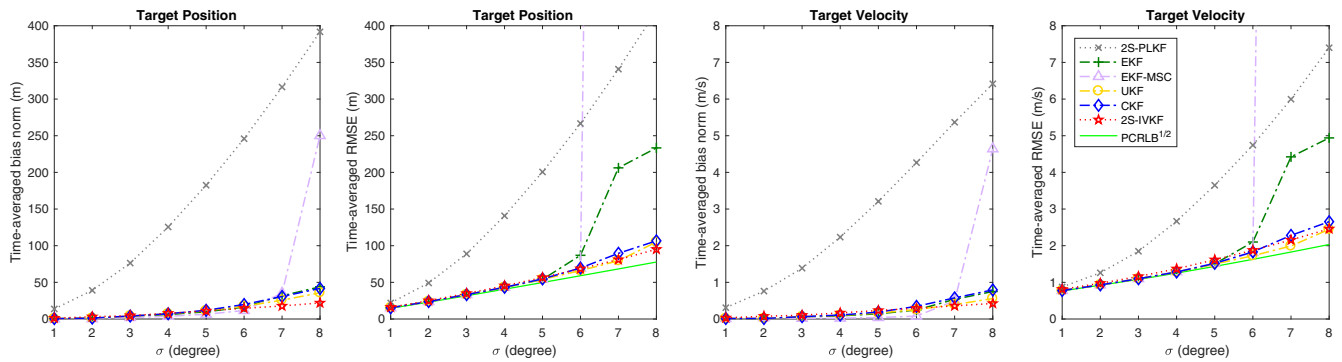


**Fig. 3.** Time-averaged bias norm and RMSE versus noise standard deviation for the 2S-IVKF in comparison with the 2S-PLKF, EKF, EKF-MS, UKF and CKF.

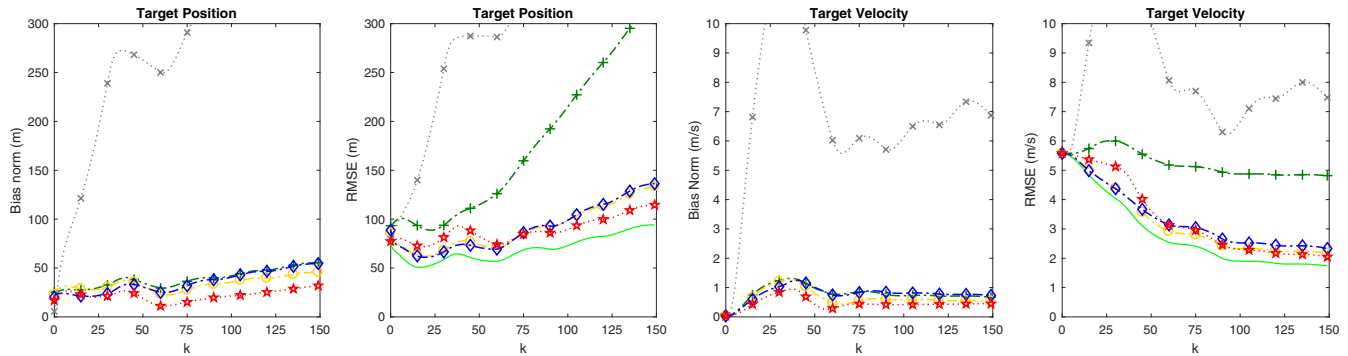


**Fig. 4.** Bias norm and RMSE over time instant  $k$  for the 2S-IVKF in comparison with the 2S-PLKF, EKF, UKF and CKF at noise standard deviation  $\sigma = 8^\circ$  (same legends as in Fig. 3). The EKF-MS diverges in this case and is excluded from comparison.

Fig. 3 compares the performance of the algorithms in terms of the time-averaged bias norm, root mean squared error (RMSE) and square root of PCRLB ( $\text{PCRLB}^{1/2}$ ), obtained from  $M=10,000$  Monte Carlo runs, for various values of noise standard deviation  $\sigma$ . The definitions of these metrics can be found in [27]. The offset parameter used in the simulations is set to  $L = 60$  to ensure that the time-averaged performance metrics are not dominated by initial tracking errors [27]. For  $\sigma \leq 5^\circ$ , the 2S-IVKF, EKF, EKF-MS, UKF and CKF exhibit a similar performance, closely attaining the PCRLB and showing almost no bias. On the other hand, the 2S-PLKF is observed to suffer from severe bias, hence producing the largest bias and RMSE among all the algorithms. As noise increases ( $\sigma > 5^\circ$ ), the EKF and EKF-MS performance degrades rapidly and their RMSEs far exceed the PCRLB. In contrast, the proposed 2S-IVKF algorithm still appears to perform well at these large noise levels by exhibiting a relatively small bias and maintaining a RMSE similar to the PCRLB. Although the UKF and CKF exhibit a comparable performance with the 2S-IVKF for  $\sigma > 5^\circ$ , they are computationally more demanding than the 2S-IVKF as observed in Table 1, where the average runtimes of the algorithms are compared.

Fig. 4 shows the bias norm and RMSE performance of the algorithms over time instant  $k$  at  $\sigma = 8^\circ$ . The EKF-MS diverges at this noise level and is excluded from comparison. In congruence with the results in Fig. 3, the 2S-PLKF exhibits the worst performance among the algorithms due to its severe bias problem. At such a large

**Table 1.** Average runtime (normalized by EKF runtime)

EKF	2S-PLKF	2S-IVKF	EKF-MS	CKF	UKF
1	1.45	1.90	3.33	6.70	7.00

noise scenario, the EKF yields a RMSE much larger than that of the 2S-IVKF, UKF and CKF. In addition, we also observe that the 2S-IVKF (although with less computation) outperforms the UKF and CKF in this case.

## 5. CONCLUSION

While enjoying low computational complexity, the recently developed 2S-PLKF algorithm [28] for 3D AOA target tracking can be plagued by severe bias problems. In this paper, we have presented a new algorithm, the 2S-IVKF, that successfully overcomes the bias problem of the 2S-PLKF. The 2S-IVKF consists of an IVKF tracker for estimating the  $xy$ -state component and a PLKF tracker for estimating the  $z$ -state component of the target. The efficacy of the 2S-IVKF was demonstrated by way of simulation examples. The 2S-IVKF was observed to outperform the EKF, EKF-MS and 2S-PLKF while performing on par with the UKF and CKF at a reduced computational complexity.

## 6. REFERENCES

- [1] V. J. Aidala, "Kalman filter behavior in bearings-only tracking applications," *IEEE Trans. Aerosp. Electron. Syst.*, vol. 15, no. 1, pp. 29–39, Jan. 1979.
- [2] V. Aidala and S. Hammel, "Utilization of modified polar coordinates for bearings-only tracking," *IEEE Trans. Autom. Control*, vol. 28, no. 3, pp. 283–294, Mar. 1983.
- [3] A. Jawahar and S. K. Rao, "Modified polar extended Kalman filter (MP-EKF) for bearings-only target tracking," *Indian J. Sci. Technol.*, vol. 9, no. 26, 2016.
- [4] M. Mallick, M. Morelande, L. Mihaylova, S. Arulampalam, and Y. Yan, *Angle-Only Filtering in Three Dimensions*, chapter 1, pp. 1–42, Wiley-Blackwell, 2014.
- [5] S. D. Gupta, J. Y. Yu, M. Mallick, M. Coates, and M. Morelande, "Comparison of angle-only filtering algorithms in 3D using EKF, UKF, PF, PFF, and ensemble KF," in *Proc. Int. Conf. Inform. Fusion*, Washington, USA, July 2015, pp. 1649–1656.
- [6] D. V. Stallard, "Angle-only tracking filter in modified spherical coordinates," *J. Guid. Control Dyn.*, vol. 14, no. 3, pp. 694–696, 1991.
- [7] S. J. Julier and J. K. Uhlmann, "Unscented filtering and nonlinear estimation," *Proc. IEEE*, vol. 92, no. 3, pp. 401–422, Mar. 2004.
- [8] E. A. Wan and R. Van der Merwe, "The unscented Kalman filter for nonlinear estimation," in *Proc. IEEE AS-SPCC*, Lake Louise, Alberta, Canada, Oct. 2000, pp. 153–158.
- [9] I. Arasaratnam and S. Haykin, "Cubature Kalman filters," *IEEE Trans. Autom. Control*, vol. 54, no. 6, pp. 1254–1269, June 2009.
- [10] A. Tloei and S. Niazi, "State estimation for target tracking problems with nonlinear Kalman filter algorithms," *Int. J. Computer Applicat.*, vol. 98, no. 17, pp. 30–36, 2014.
- [11] W. P. Wang, S. Liao, and T. W. Xing, "The unscented Kalman filter for state estimation of 3-dimension bearing-only tracking," in *Proc. ICIECS*, Wuhan, China, Dec. 2009, pp. 1–5.
- [12] R. Yang, G. W. Ng, and Y. Bar-Shalom, "Bearings-only tracking with fusion from heterogenous passive sensors: ESM/EO and acoustic," in *Proc. Int. Conf. Inform. Fusion*, July 2015, pp. 1810–1816.
- [13] X. Lin, T. Kirubarajan, Y. Bar-Shalom, and S. Maskell, "Comparison of EKF, pseudomeasurement, and particle filters for a bearing-only target tracking problem," in *Proc. SPIE Conf. Signal Data Process. Small Targets*, Orlando, FL, Aug. 2002, vol. 4728, pp. 240–250.
- [14] D. C. Chang and M. W. Fang, "Bearing-only maneuvering mobile tracking with nonlinear filtering algorithms in wireless sensor networks," *IEEE Syst. J.*, vol. 8, no. 1, pp. 160–170, Mar. 2014.
- [15] S. J. Godsill, J. Vermaak, W. Ng, and J. F. Li, "Models and algorithms for tracking of maneuvering objects using variable rate particle filters," *Proc. IEEE*, vol. 95, no. 5, pp. 925–952, May 2007.
- [16] F. Daum, "Nonlinear filters: beyond the Kalman filter," *IEEE Aerosp. Electron. Syst. Mag.*, vol. 20, no. 8, pp. 57–69, Aug. 2005.
- [17] A. Miller and B. Miller, "Tracking of the UAV trajectory on the basis of bearing-only observations," in *Proc. IEEE Conf. Decision, Control*, Los Angeles, CA, Dec. 2014, pp. 4178–4184.
- [18] B. Miller, K. Stepanyan, A. Miller, K. Andreev, and S. Khoroshenkikh, "Optimal filter selection for UAV trajectory control problems," in *Proc. Conf. Inform. Technol., Syst.*, Sept. 2013, pp. 327–333.
- [19] K. Dogancay, "3D pseudolinear target motion analysis from angle measurements," *IEEE Trans. Signal Process.*, vol. 63, no. 6, pp. 1570–1580, Mar. 2015.
- [20] A. G. Lingren and K. F. Gong, "Position and velocity estimation via bearing observations," *IEEE Trans. Aerosp. Electron. Syst.*, vol. 14, no. 4, pp. 564–577, July 1978.
- [21] N. H. Nguyen and K. Dogancay, "Multistatic pseudolinear target motion analysis using hybrid measurements," *Signal Process.*, vol. 130, pp. 22–36, Jan. 2017.
- [22] N. H. Nguyen and K. Dogancay, "Single-platform passive emitter localization with bearing and Doppler-shift measurements using pseudolinear estimation techniques," *Signal Process.*, vol. 125, pp. 336–348, Aug. 2016.
- [23] K. C. Ho, "Bias reduction for an explicit solution of source localization using TDOA," *IEEE Trans. Signal Process.*, vol. 60, no. 5, pp. 2101–2114, May 2012.
- [24] Y. Wang and K. C. Ho, "An asymptotically efficient estimator in closed-form for 3-D AOA localization using a sensor network," *IEEE Trans. Wireless Commun.*, vol. 14, no. 12, pp. 6524–6535, Dec. 2015.
- [25] N. H. Nguyen and K. Dogancay, "Computationally efficient IV-based bias reduction for closed-form TDOA localization," in *Proc. IEEE Int. Conf. Acoust., Speech, Signal Process.*, Calgary, AB, Canada, Apr. 2018, pp. 3226–3230.
- [26] V. J. Aidala and S. C. Nardone, "Biased estimation properties of the pseudolinear tracking filter," *IEEE Trans. Aerosp. Electron. Syst.*, vol. 18, no. 4, pp. 432–441, July 1982.
- [27] N. H. Nguyen and K. Dogancay, "Improved pseudolinear Kalman filter algorithms for bearings-only target tracking," *IEEE Trans. Signal Process.*, vol. 65, no. 23, pp. 6119–6134, Dec. 2017.
- [28] S. Xu, K. Dogancay, and H. Hmam, "3D pseudolinear Kalman filter with own-ship path optimization for AOA target tracking," in *Proc. IEEE Int. Conf. Acoust., Speech, Signal Process.*, Shanghai, China, Mar. 2016, pp. 3136–3140.
- [29] Y. Bar-Shalom, X. Rong Li, and T. Kirubarajan, *Estimation with Applications to Tracking and Navigation: Theory Algorithms and Software*, John Wiley & Sons, New York, 2001.
- [30] H. L. Van Trees, K. L. Bell, and Z. Tian, *Detection Estimation and Modulation Theory, Part I: Detection, Estimation, and Filtering Theory*, Wiley, New Jersey, 2nd edition, 2013.
- [31] P. Tichavsky, C. H. Muravchik, and A. Nehorai, "Posterior Cramer-Rao bounds for discrete-time nonlinear filtering," *IEEE Trans. Signal Process.*, vol. 46, no. 5, pp. 1386–1396, May 1998.